NH and CN radical emission from corona post discharge region in high density nitrogen plasma

IOP Conf. Series: Materials Science and Engineering **509** (2019) 012084 doi:10.1088/1757-899X/509/1/012084

NH and CN radical emission from corona post discharge region in high density nitrogen plasma

Muhammad Nur[1,2,*], Nelly Bonifaci[3], Andre Denat[3], Vlademir M. Atrazhev[4]

[1] Center for Plasma Research, Faculty of Science and Mathematics, Diponegoro University, Semarang
[2] Physics Department, Faculty of Science and Mathematics, Diponegoro University, Semarang
[3] G2E.Laboratory, CNRS and Joseph Fourier University 25 rue des Martyrs, 38042 Grenoble, France
[4] Joint Institute for High Temperatures (JIHT and Russian Academy of Sciences, Izhorskaya St. 13, 2125412, Moscow, Russia
***** Corresponding author: m.nur@undip.ac.id

Abstract. The corona post discharge region in high-density nitrogen plasma has been investigated. We observed the emission band (0-0) of NH located at 336 nm corresponding to the transition $A^3\prod$-$X^3\sum^-$ which is particularly intense at low pressure. The possibility would be that NH is formed from a radiative recombination between a hydrogenated compound present in trace amounts (as C_mH_n) and nitrogen. Outside the (0-0) NH band, only the band (1-1) at 337.00 nm (i.e. 1 nm from the previous one) was detected. Since its transmission probability is lower than that of the band (0-0) and is located very close to the intense $2S^+$ band (0-0) (337.13 nm), detection is not possible. A very weak emission of the CN violet system (($B^2\sum^+$-$X^2\sum$) has been identified in the discharge zone with excitation threshold in the order of 3.37 eV. The most intense bands are between 385 nm and 388.34 nm. This radical can only come from a reaction in the discharge between the nitrogen and an organic compound of the CnHm type. Although the purification system is very sophisticated, traces of hydrocarbons can be introduced either by contamination by oil vapours from the pumping system or by their presence in the starting gas (0.01 ppm). The radical CN is observed only with a discharge in negative polarity.
Keywords: Corona, post discharge region, CN violet system, nitrogen plasma, emission NH

1. Introduction

Non thermal plasmas in air and nitrogen present considerable interest for a wide range for industrial applications, such as air pollution control, waste water cleaning, bio-decontamination and sterilization, material and surface treatment, electromagnetic wave shielding, carbon beneficiation and nanotube growth, and element analysis [1]. Non thermal plasmas can be developed by corona discharge [2-4], dielectric barrier discharge [5, 6], jet plasma jet [7] and radio frequency [8]. The study of corona discharge in nitrogen gas from the electrical aspects and spectroscopic studies has been done [2]. Those studies are very focused on the discharge area. In the region post-discharge, we found still very few studies are conducted. This region contains many reactive oxygen species (ROS) and reactive nitrogen species (RNS). These radicals provide a special attraction because they can be applied in various fields as mentioned above [1, 9]. Generally, plasma species are electrons, ions, radicals, and light. Radicals are very important to induce physiological output in cells/tissues. These two types of radicals have a

significant impact on cellular physiology. Some diseases have been associated with increased levels of oxidative stress [10]. Many antioxidants induce antitumor, anti-inflammatory and antibacterial activity. Natural antioxidant intake reduces the risk of cancer, diabetes, and other diseases. Cancer cells produce increased levels of ROS, and this cancer cell property can be used for therapeutic benefits. ROS damages cancer cells and causes cell death, while normal cells tolerate the same level of ROS. It can be concluded that, pro-oxidants that induce oxidative stress, such as non-thermal plasma, may have the potential as chemotherapy [10]. Corona discharge in air or nitrogen gas, in certain condition can produced radicals such as O_3, H_2O_2, NH, CN, OH, NO [11, 12]. Radical emission from plasma has been studied by many groups [12] examines the CN emitted by carbon-carbon in the nitrogen environment. Carbon plasmas generated by pulse lasers reach energy densities of 35 J/cm^2. This paper discusses emissions from high pressure nitrogen corona discharge. The study focused on NH and CN emissions. These radical emissions are detected in several positions with very precise distances from point electrodes.

2. Methods

Experimental system for this research is shown in Fig. 1. Spectroscopy equipment consisted of the lens Spectrosil B which serves to focus the light emission from the plasma into the slit (25 mm) of a spectrograph with medium resolution HRS Jobin-Yvon. The corona discharge reactor can be moved towards the vertical and horizontal position.

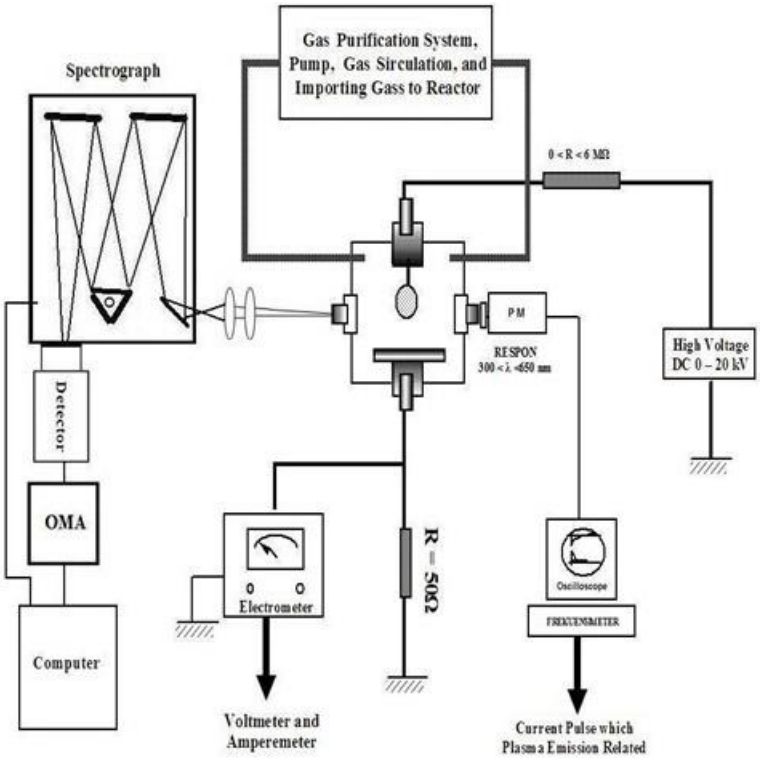

Figure 1. Scheme series of experiments.

By this movement, the slit can be placed at specific locations of the emissions. Spectrograph with a focal length of 600 mm equipped with a number of gratings 1200 grooves per mm with maximum resolution 0.20 nm. Output of Spectrograph through one slit is connected with a photodiode detector or CCD (model LN/CCD-512 SF & SB, Princeton Instruments, Inc.). The detector is connected to an EG & G Optical Multichannel Analyser (OMA) which has a spectral range between 200-850 nm (model 1460 EG & G Princeton Applied Research). To reduce the parasitic beam, detector was cooled at a temperature of -40^{o}C. Simultaneously performed well gas discharge current measurements in the reactor

with an electrometer Keithley (model 610C), and voltage can be read directly from a DC generator RHSR/20PN60 Spellman. In addition to the above, the light emission was also detected through the help photo-multiplicator (Dario 56AVP model) which has a spectral response between 300 and 650 nm. Current pulse was detected with a Tektronix oscilloscope (model 7633).

Discharge and Post Discharge Region. The image of the tip is focused on the entrance slot of the monochromator using a pair of plano-convex lenses in quartz. The set of lenses allows us to have an image of the light zone that is of the same order of magnitude as the original. By horizontal and vertical displacement of the whole of the cell, it is possible to focus in the entrance slot of the monochromator a small portion of the light zone located at a distance X from the point**.** Setting the position of the point electrode horizontally can be seen in the illustration shown by Fig. 2.

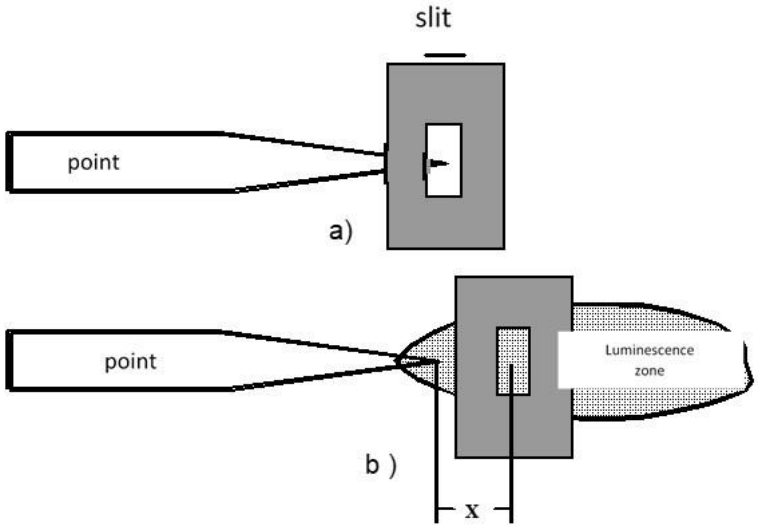

Figure 2. Position of the slot with respect to the tip. Adjustable entrance slot from 10 μm to 3 mm. a) Focusing the tip on the entrance slit b) Position of the entrance slit in the light zone. A small part of this area can be analysed.

3. Results and Discussion

3.1. Emission in the Discharge Zone

In the discharge zone, the light emitted by the cold plasma formed during a corona discharge in nitrogen gas was devoted to the exploited. The majority of the spectra that we present and analyse were obtained in cathode point with continuous glow discharges. Emission spectrum of molecular nitrogen is shown in Fig. 3. In this regime, as in the case of nitrogen high density, two different zones can be distinguished: the ionization zone defined by P_∞, Tp and Np and the transport zone defined by T_∞, P_∞ and N_∞. As the density of the luminescent medium is not known a priori, we will use the density N_∞ to present the results. All observations on the emitted light, in the wavelength range 200 nm-900 nm, show the presence of the following emission bands. The second positive system ($C^3\prod u$-$B^3\prod g$), the first negative system ($B^2\sum^+ u$-$X^2\sum^+ g$), the first positive system ($B^3\prod g$-$A^3\sum^+ u$), and the fourth positive system ($D^3\sum^+ u$-$B^3\prod g$).

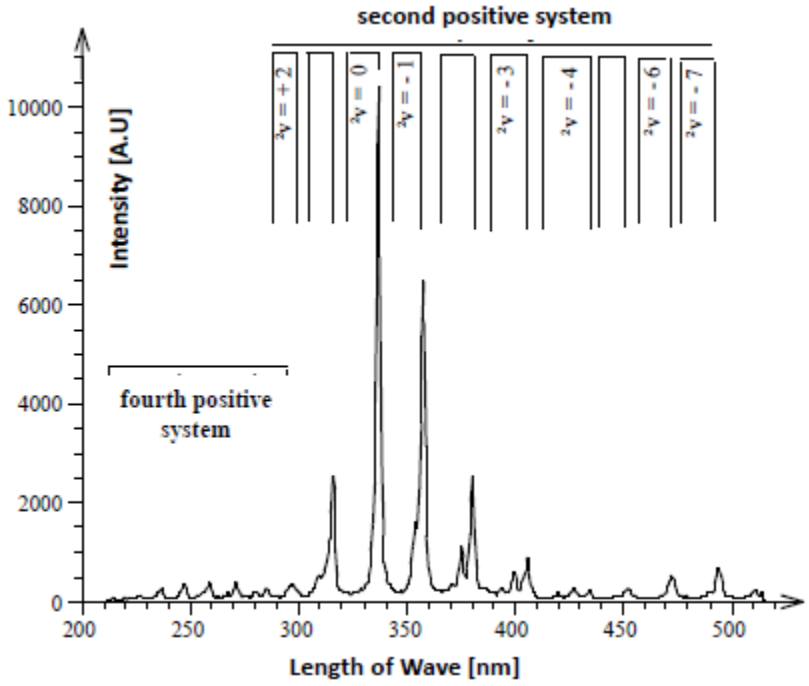

Figure 3. Emission spectrum of molecular nitrogen in the spectral window 200 nm-550 nm, P_{∞}=0,5 MPa, with acquisition time t_a=1 s and discharge current I_{dich}=1,4 mA. Spectrograph Jarrell-Ash with grade of 150 lines/mm.

There are several physical processes that occur in the post-discharge zone. The first, in this zone the temperature drops, and also the active species and electron densities decreases, and the emission intensity decreases sharply. This leads to the appearance of the second non-luminous zone where the radiation process is quasi-absences and active species reach their minimum density. Furthermore, the temperature continues to decrease, a transfer phenomenon will appear between the basic state N_2 molecules that produce active new formations species such as: N_2 (A), N_2, and high vibration nitrogen ground-state molecules. The third zone, called the end of glow discharge, that emission of N_2 positive system completely disappears and this zone mainly characterized by the emission of the dominant CN violet and NH. The interaction of active species of nitrogen with hydrocarbon vapours causes the emergence of large flower compounds for plasma chemical post-disposal processes. Among all these reactions products play an important role in the CN violet spectral systems and NH 336 nm systems. The RNS in our post-discharge can be explained is caused by the presence of traces of hydrocarbons in the experimental reactor even though the amount is very small.

3.2. The 336 nm system of NH

In all tests, we observed the presence of a localized band on the R branches of the $2S^+$ band (0-0) at the position of point in the 2.60 mm (Fig. 4). At the position of 2.65 mm we detected emission of NH. This emission can be attributed to the band (0-0) of NH located at 336 nm (Fig. 5) corresponding to the transition $A^3\Pi$-$X^3\Sigma^-$ which is particularly intense at low pressure [13]. The origin of this band is not clear. One possibility would be that NH is formed from a radiative recombination between a hydrogenated compound present in trace amounts (as CmHn) and nitrogen [14]. Outside the (0-0) NH band, only the band (1-1) at 337.00 nm (i.e. 1 nm from the previous one) was detected. Since its transmission probability is lower than that of the band (0-0) and is located very close to the intense $2s^+$

band (0-0) (337.13 nm), detection is not possible. This is what causes emission at 337.13 nm to be undetected after the detector position shifts from 2.65 mm to 2.66 mm (Fig. 6), and position of 2.67 mm (Fig. 7).

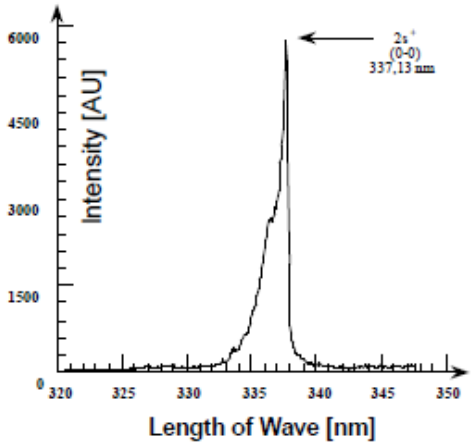

Figure 4. The emission of transition (0-0) of $2s^+$ nitrogen. P_∞=1 MPa. The acquisition was made on a position at 2.60 mm from the point with ta=1 sec. Jobin-Yvon Spectrograph, with grade of 1200 lines/mm.

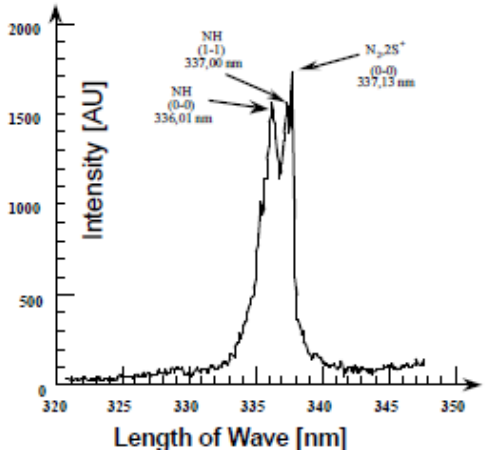

Figure 5. Demonstration of the emission of the transition (0-0) and (1-1) of NH on the rotational structure of the 2S+band (0-0). The acquisition was made on a position at 2.65 mm from the point, ta=1 sec and P_∞=1 MPa. Jobin-Yvon Spectrograph, with grade of 1200 lines/mm.

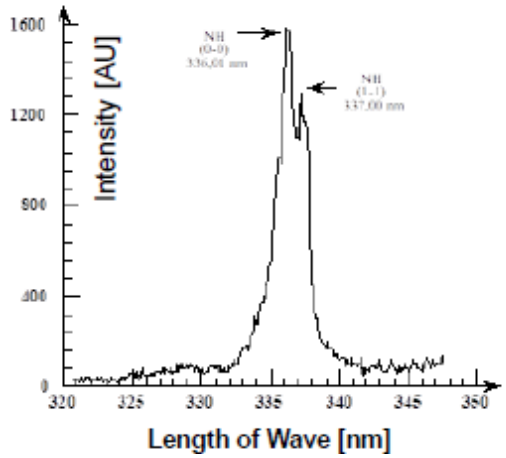

Figure 6. The emission of the (0-0) and (1-1) transition of the NH molecules at the 2.66 mm position from the tip. ta=1 sec and P∞=1 MPa. Jobin-Yvon Spectrograph, with grade of 1200 lines/mm.

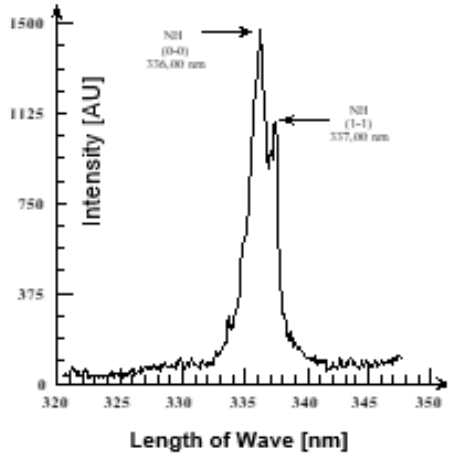

Figure 7. The emission of the transition (0-0) and (1-1) of the NH molecule at the position 2.67 mm from the tip. ta=1 sec and P∞=1 MPa. Jobin-Yvon Spectrograph, with grade of 1200 lines/mm.

Remarkably, Fig. 4, 5, 6 and 7 show that the emission of the NH molecule becomes detectable (i.e. of an intensity comparable to that of the 0-0 band of $2s^+$) that if the entrance slot of the spectrograph (width 25 μm) analyses the emitted light at a distance L greater than 2.60 mm from the tip. For L <2.6 mm, only the band (0-0) of $2s^+$ appears. At a distance L=2.65 mm (only 50 μm later), the transitions (0-0) and (1-1) of NH start to emerge, the emission (0-0) of the $2s^+$ being always observed although with an intensity three times lower.

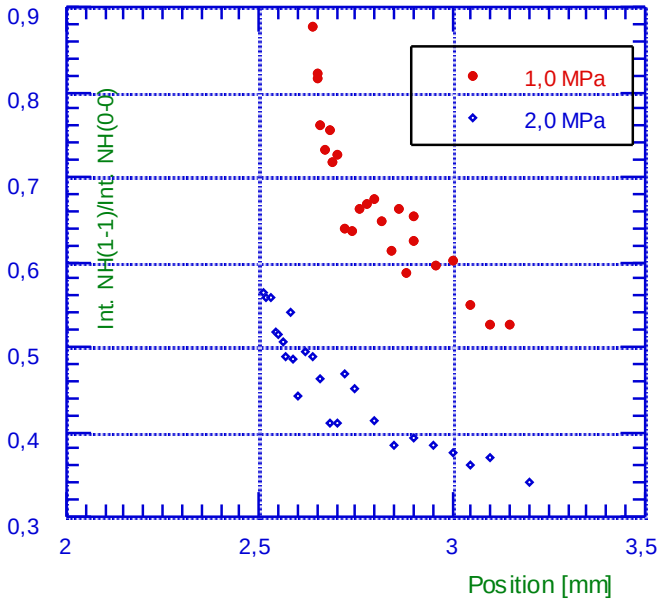

Figure 8. Evolution of the ratio of the intensity of the transition (1-1) on the intensity of the transition (0-0) of NH with the position in the post-discharge zone.

At the 2.66 mm position of the tip, the transition band head (0-0) of the $2s^+$ has completely disappeared and all that remains is the emission of NH. From this result, we can estimate the length of the glow discharge zone (defined by an emission due essentially to N_2^*) and, beyond this zone, where only the emission of radicals is detected (like NH), the length of the area we will call post-discharge area. We plot in Fig. 8, the curves of the ratios between the intensity of the headband (1-1) of NH and the intensity of the headband (0-0) of NH depending on the position L and for two different pressures, P_∞=1 MPa and 2 MPa. The ratio of the intensity of the transition (1-1) on the intensity of the transition (0-0) for two gas pressures indicates that the population of NH molecules with a transition (1-1) at lower pressures (1 MPa) is easier to form compared to the pressure 2 MPa. The ratio of two systems indicated that pressure 1 MPa is 1.5 times the ratio at the pressure of 2 MPa. It can be explained that energetic particles such as electrons and ions have more energy, so that energy transfer when colliding gives impact for higher molecular excitation levels.

3.3. The Violet system of CN

A very weak emission of the CN violet system (B2Σ+-X2Σ) has been identified in the discharge zone (excitation threshold in the order of 3.37 eV [15]. The most intense bands are between 385 nm and 388.34 nm (see for example Fig. 9 and 10). This radical can only come from a reaction in the discharge between the nitrogen and an organic compound of the CnHm type [14]. Although the purification system is very sophisticated, traces of hydrocarbons can be introduced either by contamination by oil vapours from the pumping system or by their presence, not eliminated, in the starting gas (0.01 ppm). The radical CN is observed only with a discharge in negative polarity. Its intensity depends on the pressure of the gas (it increases with P∞) but especially on the filling mode of the test cell.

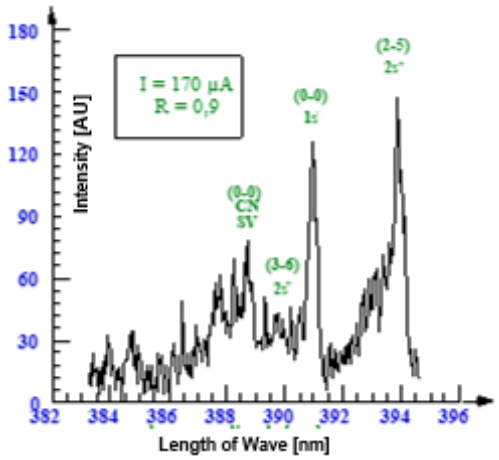

Figure 9. Spectrum of bands (0-0) of $1s^-$ and (2-5) of $2s^+$, for N_∞=2.4 10^{20} cm^{-3}) and I_{disch}=170 µA. ta=1 sec.

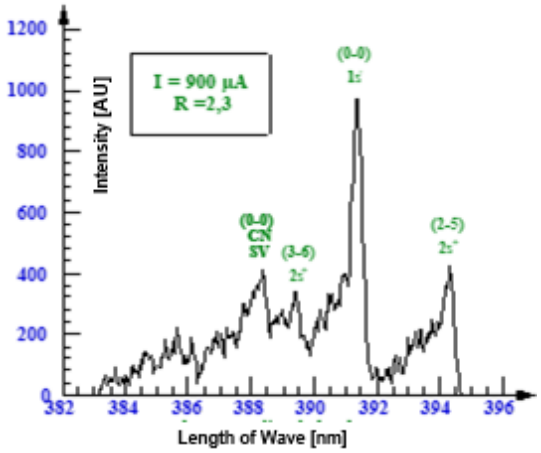

Figure 10. Spectrum of bands (0-0) de $1s^-$ et (2-5) de $2s^+$, for N_∞=2.4 10^{20} cm^{-3}, I_{disch}=900 µA and the acquisition time of t_a=1 sec.

The emission bands of the CN violet system $B^2\Sigma^+$-$X^2\Sigma^+$ were detected over a distance of 3 to 4 mm, after the ionization zone or drive zone. The formation of the CN violet system is due to the reactions of the active nitrogen atom with organic compounds. This formation is produced by the following three-body recombination [14]:

$$C + N + M \text{ ----> } CN(B^2\Sigma^+) + M$$

This therefore requires the dissociation of the nitrogen molecule in the discharge followed by the three-body recombination.

4. Conclusion

Corona plasma is classically known to consist of two zones, an ionization zone and a charge flow zone. In this study the plasma species aspects can clearly distinguish two zones, namely plasma laminate area and plasma post-discharge. We detected clearly the formation of NH and CN radicals is in the post discharge plasma region. In this study NH radicals were detected through emission that can be attributed to the band (0-0) of NH located at 336 nm corresponding to the transition $A^3\Pi$-$X^3\Sigma^-$**.** The spatial study of the distribution of the nitrogen and radical emission bands allowed us to distinguish and analyse the two zones of a corona discharge in a dense gas. The ionization zone characterized by the existence of excited state bands of nitrogen (N_2*) and ionized nitrogen (N_2^+*). The transport zone where the previous bands are absent and where bands of NH* and CN* radicals appear showing the existence of chemical reactions between the species produced in the plasma.

Acknowledgments

M. Nur thanks to the Ministry of Research Technology and Higher Education on the facilities provided in the implementation of Higher Education Innovations in 2017. This project facilitated the development of plasma science and technology in Indonesia.

References

[1] Mizuno A 2007 Industrial applications of atmospheric non-thermal plasma in environmental remediation *Plasma Phys. Contr. F.* **49** 5A A1

[2] Nur M 1997 *Etudes des decharges couronne dans l'argon et l'azote tres purs: transport des charges, spectroscopie et influence de la densite* Université Joseph Fourier (Grenoble)

[3] Nur M, Bonifaci N and Denat A 2014 Ionic wind phenomenon and charge carrier mobility in very high density argon corona discharge plasma *J. Phys. Conf. Ser.* **495** 012041
[4] Dau V T, Dinh T X, Terebessy T and Bui T T 2016 Bipolar corona discharge based air flow generation with low net charge *Sens. Actuators A Phys.* **244** 146-55
[5] Kogelschatz U, Eliasson B and Egli W 1997 Dielectric-barrier discharges. Principle and applications *Le Journal de Physique IV* **7** C4 C4-47-C4-66
[6] Nur M, Amelia Y A, Arianto F, Kinandana A W, Zahar I, Susan A I and Wibawa J P 2017 Dielectric Barrier Discharge Plasma Analysis and Application for processing palm oil mill effluent (POME) *Procedia Eng.* **170** 325-31
[7] Nakajima Y, Mukai K, Rahayu H S E, Nur M, Ishijima T, Enomoto H, Uesugi Y, Sugama J and Nakatani T 2014 Cold plasma on full-thickness cutaneous wound accelerates healing through promoting inflammation, re-epithelialization and wound contraction *Clin. Plasma Med.* **2** 1 28-35
[8] Kiristi M, Bozduman F, Oksuz A U, Hala A and Oksuz L 2015 A comparison study of microwave and radio frequency plasma polymerized PEDOT thin films *J. Macromol. Sci. A* **52** 2 124-9
[9] Machala Z, Janda M, Hensel K, Jedlovský I, Leštinská L, Foltin V, Martišovitš V and Morvova M 2007 Emission spectroscopy of atmospheric pressure plasmas for bio-medical and environmental applications *J. Mol. Spectrosc.* **243** 2 194-201
[10] Tanaka H and Hori M 2017 Medical applications of non-thermal atmospheric pressure plasma *J. Clin. Biochem. Nutr.* **60** 1 29-32
[11] Ciobotaru L and Gruia I 2015 Study of the carbon atoms production in methanol/ethanol–nitrogen flowing post-discharge plasma *Rom. J. Phys.* **60** 9-10 1536-49
[12] Abdelli-Messaci S, Kerdja T, Bendib A and Malek S 2005 CN emission spectroscopy study of carbon plasma in nitrogen environment *Spectrochim. Acta Part B At. Spectrosc.* **60** 7-8 955-9
[13] Pearse R W B and Gaydon A G 1976 *Identification of molecular spectra*: Chapman and Hall)
[14] Iwai T, Savadatti M and Broida H 1967 Mechanisms of populating electronically excited CN in active nitrogen flames *J. Chem. Phys.* **47** 10 3861-74
[15] Washida N, Kley D, Becker K and Groth W 1975 Experimental study of the C (3 P)+ N (4 S)+ M→ CN (B 2Σ+)+ M recombination *J. Chem. Phys.* **63** 10 4230-41